

acids by the parallel and alternating synthesis of two polymer chains. The ability to decipher non-natural components in a library by Edman sequencing circumvents the potential problem of identifying non-natural biopolymers and should therefore allow for the inclusion of a wide variety of novel building blocks and conformational constraints in a diverse ligand library.

Acknowledgment. The authors would like to thank Scott Chamberlain for Edman sequencing; Dr. Reyna Simon and Robert Kania for providing various non-natural monomers; and Sean O'Connell, Dr. Fred Cohen, Dr. Frank Masiarz, Dr. Charles Marlowe, and Dr. Walter Moos for helpful discussions.

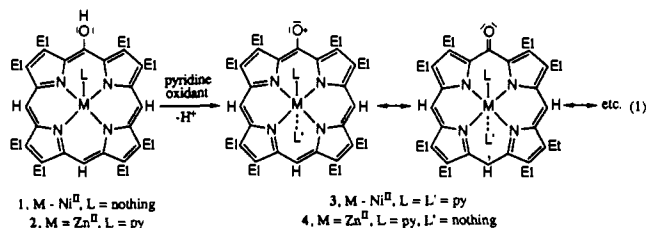
Carbon-Carbon Bond Formation in the Dimerization of (Octaethylxophlorin radical)nickel(II)

Alan L. Balch,* Bruce C. Noll, Steven M. Reid, and Edward P. Zovinka

Department of Chemistry
University of California
Davis, California 95616

Received November 30, 1992

Metalloporphyrin π -cation radicals are significant intermediates in biological oxidations that are catalyzed by heme enzymes.¹ Related iron oxophlorin π -radicals may be involved as intermediates in heme catabolism.² Evidence for the dimerization of both classes of π -radicals has been reported.³⁻⁶ Recent structural studies of the products of one-electron oxidation of $\{\text{Ni}^{\text{II}}(\text{OEP})\}$ and $\{\text{Zn}^{\text{II}}(\text{OEP})\}$ (OEP is octaethylporphyrin dianion) have shown that these crystallize as the dimers $[\text{Zn}(\text{OEP}^*)(\text{H}_2\text{O})_2(\text{ClO}_4)_2]$ and $[\text{Ni}(\text{OEP}^*)_2(\text{ClO}_4)_2]$.^{4,5} These form tight, cofacial dimers in which the interplanar separation is 3.31 Å for the zinc complex and 3.19 Å for the nickel complex. While these dimers are diamagnetic, classical single bonds between any of the constituent atoms are absent. Octaethylxophlorin (or *meso*-hydroxyoctaethylporphyrin, H_2OEPO) reacts with divalent metal ions (Zn(II), Ni(II)) to form complexes $\{\text{L}\}_n\text{M}^{\text{II}}(\text{OEPOH})$, **1**, in which a free exocyclic hydroxyl group is present.^{7,8} In pyridine (py) solution these are readily oxidized by one electron to form air stable radicals with the loss of a proton as shown in eq 1. These radicals



crystallize from pyridine solution as monomeric species. The nickel complex, **3**, $\{(\text{py})_2\text{Ni}(\text{OEPO}^*)\}$, has two axial ligands that prevent

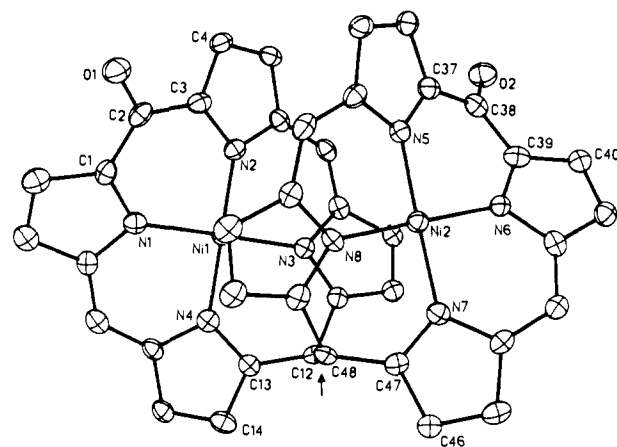
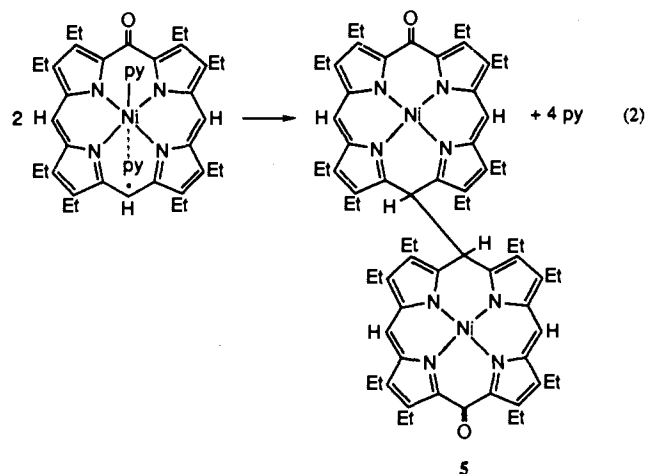


Figure 1. A view of $\{\text{Ni}^{\text{II}}_2(\text{OEPO})_2\}$ with the ethyl groups omitted for clarity. This view looks down on the planes of the two macrocycles and shows 50% thermal contours. The arrow points to the C(12)-C(48) bond, which connects the two macrocycles. Selected bond lengths (Å): C(12)-C(48), 1.614(8); Ni(1)-N(1), 1.910(5); Ni(1)-N(2), 1.904(4); Ni(1)-Ni(3), 1.920(5); Ni(1)-N(4), 1.912(4); Ni(2)-N(5), 1.918(4); Ni(2)-N(6), 1.912(5); Ni(2)-N(7), 1.924(4); Ni(2)-N(8), 1.912(5); C(2)-O(1), 1.249(8); C(38)-O(2), 1.236(7). Selected bond angles (deg): C(11)-C(12)-C(13), 110.9(4); C(11)-C(12)-C(48), 113.0(4); C(13)-C(12)-C(48), 110.0(5); C(12)-C(48)-C(47), 107.1(5); C(12)-C(48)-C(49), 115.6(4); C(47)-C(48)-C(49), 112.1(4); N(1)-Ni-N(3), 177.4(2); N(2)-Ni(1)-N(4), 176.7(2); N(5)-Ni(2)-N(7), 175.9(2); N(6)-Ni(2)-N(8), 179.0(2).

close approach to another molecule.⁸ The zinc complex **4** is five-coordinate but crystallizes with an additional, unbound pyridine in the lattice.⁷ This also appears to prevent interaction between the radicals in the solid state. However, evidence for the dimerization of $\text{Ni}(\text{OEPO}^*)$ in chloroform solution has been reported, but no structure was suggested.⁶ We now report on the structure of the dimeric form of the nickel radical, $\{\text{Ni}_2(\text{OEPO})_2\}$, **5**, which forms by eq 2.



Crystallization of $\{(\text{py})_2\text{Ni}(\text{OEPO}^*)\}$, **3**, from dichloromethane/95% ethanol yields red crystals of **5** which are morphologically distinct from **3**. The results of an X-ray crystallographic examination of **5**, $\{\text{Ni}_2(\text{OEPO})_2\}$, are given in Figures 1 and 2.⁹ Figure 1 gives the numbering system and shows how the two macrocycles lie over one another in an offset manner. Figure 2 shows a stereoscopic view. The macrocycles are connected by a carbon-carbon bond between the two meso carbons, C(12) and C(48), which lie opposite (or para) to the oxygenated carbons. The new C-C bond distance is long (1.614(8) Å), but it is clearly

(1) Ortiz de Montellano, P. R., Ed. *Cytochrome P450*; Plenum Press: New York, 1986. Everse, J.; Everse, K. E.; Grinsham, M. B., Eds. *Peroxidases in Chemistry and Biology*; CRC Press: Boca Raton, FL, 1991.

(2) Bissell, D. M. In *Liver: Normal Function and Disease. Vol. 4, Bile Pigments and Jaundice*; Ostrow, J. D., Ed.; Marcel Dekker, Inc.: New York, 1986; p 133. Schmid, R.; McDonagh, A. F. In *The Porphyrins*; Dolphin, D., Ed.; Academic Press: New York, 1979; Vol. 6, p 258. O'Carra, P. In *Porphyrins and Metalloporphyrins*; Smith, K. M., Ed.; Elsevier: New York, 1975; p 123.

(3) Fuhrhop, J.-H.; Wasser, P.; Riesner, D.; Mauzerall, D. *J. Am. Chem. Soc.* **1972**, *94*, 7996.

(4) Song, H.; Reed, C. A.; Scheidt, W. R. *J. Am. Chem. Soc.* **1989**, *111*, 6867.

(5) Song, H.; Orosz, R. D.; Reed, C. A.; Scheidt, W. R. *Inorg. Chem.* **1990**, *29*, 4274.

(6) Fuhrhop, J.-H.; Besecke, S.; Subramanian, J.; Mengersen, Chr.; Riesner, D. *J. Am. Chem. Soc.* **1975**, *97*, 7141.

(7) Balch, A. L.; Noll, B. C.; Zovinka, E. P. *J. Am. Chem. Soc.* **1992**, *114*, 3380.

(8) Balch, A. L.; Noll, B. C.; Zovinka, E. P. Submitted for publication.

(9) Red trigonal prisms of $\{\text{Ni}_2(\text{OEPO})_2\} \cdot 2\text{CH}_2\text{Cl}_2$, $\text{C}_{74}\text{H}_{60}\text{Cl}_2\text{N}_8\text{Ni}_2\text{O}_2$, crystallize in the monoclinic space group $P2_1/n$ with $a = 14.782(3)$ Å, $b = 26.774(5)$ Å, $c = 18.073(4)$ Å, and $\beta = 105.97(3)^\circ$ at 123 K with $Z = 4$. Refinement of 5836 reflections with $F > 6.0\sigma(F)$ and 807 parameters gave $R = 0.058$, $R_w = 0.067$.

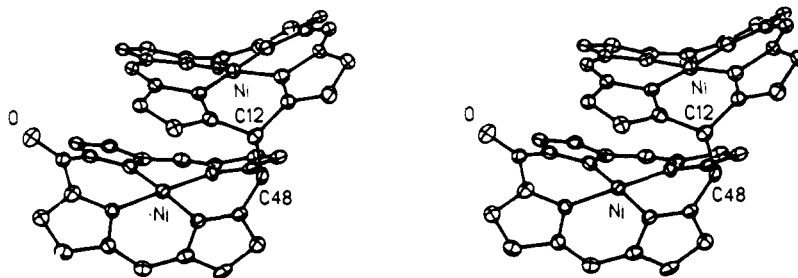


Figure 2. A stereoscopic view of $\{Ni^{II}_2(OEPO)_2\}$.

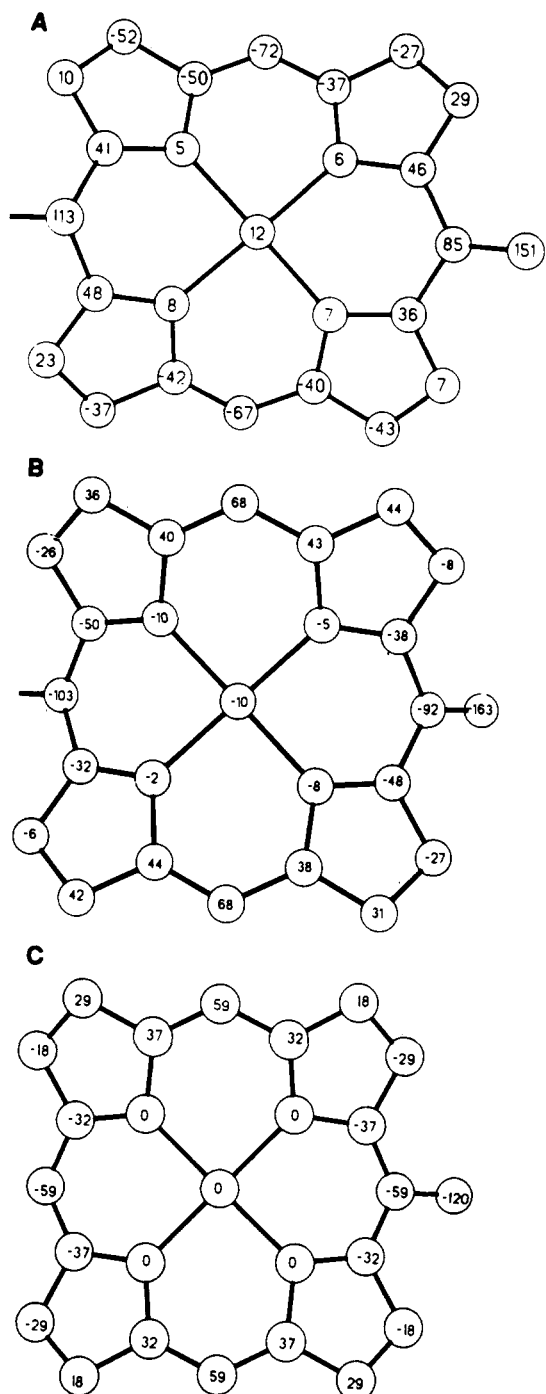


Figure 3. Diagrams of the macrocycles in $\{Ni_2(OEPO)_2\}$ (**5**; A and B) and $Ni^{II}(OEPOH)$ (C). Each atom label has been replaced by a number that represents the perpendicular displacement (in 0.01 Å) from the plane of the macrocycle.

indicative of a localized bond. This localized bonding contrasts sharply with the structure of the cofacial porphyrin π -cation

radicals in $[(OEP^*)Ni]_2(ClO_4)_2$. The bond angles at the two meso carbon junctions range from 107.1° to 115.6° and do not appear to indicate any unusual angular strain. The two macrocycles are clearly nonplanar, as the stereoview shows. The magnitude of the saddle-shaped distortion can be seen in Figure 3, where it is compared to that of $Ni^{II}(OEPOH)$.⁸ These distortions are, in part, a result of the small size of the Ni(II) ion. The eight independent Ni–N distances cover a narrow range (1.904–1.924 Å). For comparison the Ni–N distance in diamagnetic $Ni^{II}(OEPO)$ is 1.921(6) Å,⁸ and in tetragonal $\{Ni^{II}(OEP)\}$ it is 1.929(3) Å.¹⁰ In six-coordinate $\{(py)_2Ni(OEPO^*)\}$, the Ni–N distances average 2.07 Å and the nickel appears to be high-spin ($S = 1$).⁸ However, the saddle distortion also facilitates the approach of the two macrocycles and the pyramidalization of the meso carbon atoms that is required for dimerization. The distortion is larger in the dimer **5** than in $\{Ni^{II}(OEPOH)\}$ or in $\{Ni^{II}(OEP)\}$.¹⁰ The two C–O distances (1.249(8) and 1.236(7) Å) are consistent with the presence of keto groups in the macrocycle. By acting as an electron reservoir, the meso oxygen functionalities promote the dimerization of the oxophlorin radicals in a fashion not possible in porphyrin radicals. Electronic structure calculations for the oxophlorin radical show that the highest regions of spin density occur at the oxo function and at the meso carbon opposite the oxo group.¹¹ Thus coupling at the γ meso carbon rather than at the β or δ meso positions is consistent with the electron distribution in the radical. The formation of **5** is reversible. Dissolution in pyridine regenerates the characteristic electronic absorption spectrum⁸ of **3**, $\{(py)_2Ni(OEPO^*)\}$.

While no structural proposals for the dimeric form of $Ni(OEPO^*)$ had been put forth,⁶ coupling through meso carbons was proposed earlier for the dimerization of metalloporphyrin π -cation radicals³ and for a dimer of dioxoporphodimethene.¹¹ None of these suggestions were supported by structural studies. Dimerization of $\{Zn(OEPO^*)\}$ has also been reported.⁶ It remains to be seen whether this dimerization occurs similarly to that of the nickel complex, and how the larger size of the zinc ion would affect the distortion of the macrocycle. The structure of **5** also contrasts with observations on the self-association of π -radicals forms of nickel(II) complexes of two tetraaza macrocycles where dimerization involves both weak Ni–Ni interactions and direct π – π overlap between macrocycles.^{13,14} Neither feature is found in **5**.

Acknowledgment. We thank the National Institutes of Health (GM 26226) for support.

Supplementary Material Available: Tables of atomic coordinates, bond distances, bond angles, anisotropic thermal parameters, hydrogen atomic coordinates, and crystal data for $\{Ni_2(OEPO)_2\} \cdot 2CH_2Cl_2$ (13 pages); listing of observed and calculated structure factors for $\{Ni_2(OEPO)_2\} \cdot 2CH_2Cl_2$ (31 pages). Ordering information is given on any current masthead page.

- (10) Meyer, E. F., Jr. *Acta Crystallogr.* **1972**, *B28*, 2162.
 (11) Morishima, I.; Fujii, H.; Shiro, Y.; Sano, S. *J. Am. Chem. Soc.* **1986**, *108*, 3858.
 (12) Fuhrhop, J.-H.; Baumgartner, E.; Bauer, H. *J. Am. Chem. Soc.* **1981**, *103*, 5854.
 (13) Peng, S.-M.; Ibers, J. A.; Millar, M.; Holm, R. H. *J. Am. Chem. Soc.* **1976**, *98*, 8037.
 (14) Peng, S.-M.; Goedken, V. L. *J. Am. Chem. Soc.* **1976**, *98*, 8500.